Analysis on the Switching Surge Characteristics of a High-Voltage Induction Motor Fed by PWM Inverter Using EMTP

Jae-Chul Kim† , Seung-Yeop Song* and Do-Hoon Lee**

Abstract - The PWM inverter drive may cause an over voltage at the motor terminal, which imposes severe electric stresses on the inter-turn insulation of motor windings. Unlike low-voltage induction motors, high-voltage induction motors have a stator type of form-wound coil for insulation and are insulated to the slot and the coil. So, this paper presents a PWM 3-level inverter, H-Bridge cascaded 7-level inverter and High-voltage induction motor model. It then analyzes the voltage that generates at the input terminal of the high-voltage induction motor fed by each inverter. Also, in order to examine a factor that influences the switching surge voltage, this paper proposes the system equivalent model and performs the case studies using EMTP.

Keywords: Cable, EMPT, High-voltage induction motor, PWM, Switching surge

1. Introduction

Recent advancement in power electronic switching devices has enabled high switching operation and has improved the performance on PWM inverters for driving induction motors. Particularly, the IGBT type inverter with the high switching frequency makes the load operation smooth in comparison with the GTO inverter. It also increases the efficiency of the motor and allows for operation with minimal noise pollution. However, the rapid rise-time and the high rate of voltage increase (*dv/dt*) of the IGBT inverter have adverse effects on the motor insulation in that the steep rising and falling pulses lead to an uneven distribution of voltage within the motor. In fact, stator winding failure of the induction motor by this voltage surge frequently occurs [1-3].

In addition, the switching surge voltage is influenced by the feeder cable between an inverter and a motor. The voltage wave through the feeder cable is twofold at the motor terminal because of the mismatch of characteristic impedance between the feeder cable and the motor.

As such, the switching surge voltage becomes the major cause of insulation failure by serious voltage stress in the stator winding of the induction motor. These switching surge characteristics are significant data needed to increase the system reliability. In this paper, it is proved that the switching surge voltage is the most important factor in high-voltage induction motor design.

† Corresponding Author: Dept. of Electrical Engineering, Soongsil University, Seoul, Korea. (jckim@ssu.ac.kr)
* Dept. of Electrical Engineering, Soongsil University, Seoul, Korea.
** LG Industrial Systems, Advanced Power Equipment Research LAB, Chungju, Korea.(dhlee@lgis.com)
Received September 9, 2004 ; Accepted December 21, 2004

2. Generation Principle of Switching Surge Voltage and Transmission Theory

2.1 Generation Principle of Switching Surge Voltage

The output voltages of the PWM inverter include many harmonic components that are caused by the switching frequency, with the exception of the fundamental components. The induction motor is driven by the fundamental wave components and other harmonic components are generated as the loss and the noise.

The peak value of output voltage is lower than DC voltage because an inverter controlled by switching devices converts AC voltage into DC voltage. The surge voltage is generated somewhat by switching at the output terminal of the inverter. Inductance L and stray capacity C exist between an inverter and a motor. The surge voltage that is amplified by LC resonance is applied to the input terminal of the motor. As well, the charging and discharging current as in Eq. (1) generates by stray capacity C [3, 4].

$$i = C\frac{dv}{dt} \tag{1}$$

This current contains high harmonic components and circulates between an inverter and a motor through a ground. Therefore, the leakage current that includes the harmonics usually results in the over-current trip. If the leakage current exceeds the rated current of the switching device, a piece of equipment may be broken. The surge voltage that is applied to the input terminal of the motor is theoretically twice as big as the peak value of the inverter output voltage.

According to the waveform rise time at the switching and considering length of the cable, the surge voltage is different. But this is an unavoidable phenomenon in the PWM mode. Fig. 1 indicates the voltage waveforms of the inverter driven induction motor system.

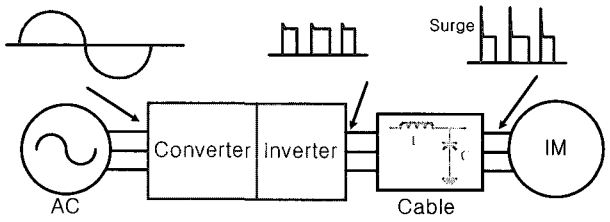

Fig. 1 Voltage waveforms of inverter driven induction motor system

2.2 Transmission theory of switching surge voltage

PWM pulse is propagated by the traveling wave of the transmission line in the cable that connects the inverter with a motor. Because the characteristic impedance of the cable is much smaller than the characteristic impedance of stator winding, total reflection happens. Moreover, the voltage of the motor terminal is twice as big as the output voltage of the inverter due to superposition of the incident wave and the reflection wave. This voltage also causes serious stress to the stator winding of the motor [3].

The surge impedance of cable (Z_C) and motor (Z_M) are provided by Eqs. (2) and (3).

$$Z_C = \sqrt{\frac{L_c}{C_c}} \tag{2}$$

$$Z_M = \sqrt{\frac{L_m}{C_m}} \tag{3}$$

where, L_C and C_C are the inductance and the capacitance of cable per length, L_m is the total motor inductance, and C_m is the capacitance of stator winding.

The reflection wave (E') is calculated by Eqs. (4) and (5) in the load side.

$$E' = \Gamma_L \times E \tag{4}$$

$$\Gamma_L = \frac{Z_M - Z_C}{Z_M + Z_C} \tag{5}$$

where, Γ_L is the reflection constant in the load side and E is the magnitude of incident wave.

The voltage reflection constant Γ_L in the load side is presented in the following three special cases [5].

a) shorted circuit : $\Gamma_L = -1,\ E' = -E$

b) open circuit : $\Gamma_L = 1,\ E' = E$

c) matching ($Z_L = Z_S$) : $\Gamma_L = 0,\ E' = 0$

The characteristic impedance of the cable is much smaller than the characteristic impedance of the motor. Therefore, if we see the circuit at the source side, that is the open circuit. If we see the circuit at the load side, that is the short circuit. Fig. 2 shows the process of voltage reflection in the open circuit [6].

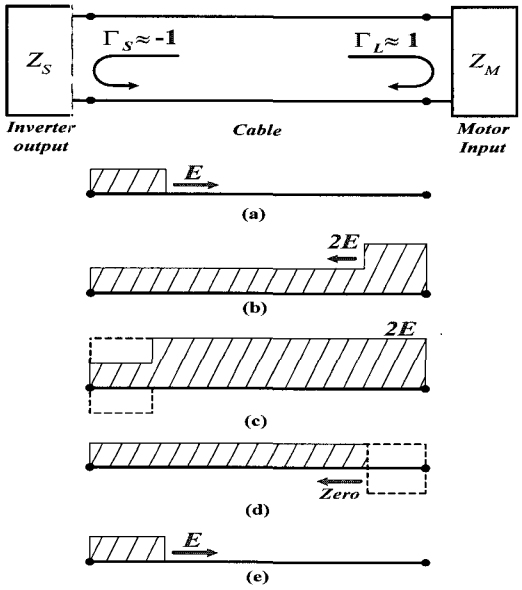

Fig. 2 Process of voltage reflection in the open circuit

The incident wave is double at the motor terminal due to reflection constant $\Gamma_L \approx 1$. When the reflection wave reaches for the source side, the reflection constant is $\Gamma_S \approx -1$. Then total voltage is E due to the negative reflection wave. When this second reflection constant reaches for the motor, the third reflection wave happens and total voltage is zero.

The propagation velocity of surge voltage that travels through the cable is given by

$$v = \frac{1}{\sqrt{L_C C_C}} = \frac{1}{\sqrt{\mu_o \varepsilon_o \varepsilon_r}} \text{ [m/s]} \tag{6}$$

The time (t_c) in which a surge voltage travels from a source side to a load side is given by Eq. (7).

$$t_c = \frac{l_c}{v} \tag{7}$$

where, l_c is the cable length.

Considering the rise-time (t_r) of input voltage, the magnitude of peak voltage at the motor terminal is as follows [7].

$$V_{peak,L-L} = \frac{3l_c E\Gamma_L}{vt_r} + E \quad (\text{If, } t_c < \frac{t_c}{3}) \tag{8}$$

$$V_{peak,L-L} = E\Gamma_L + E \quad (\text{If, } t_c \geq \frac{t_c}{3}) \tag{9}$$

3. Modeling of ASD System and Harmonic Spectrum Analysis

EMTP is the electromagnetic transient analysis program, which is developed to analyze the transient steady state of a power system. It is also able to analyze the dynamic characteristic of the total system, individual devices and harmonics [8].

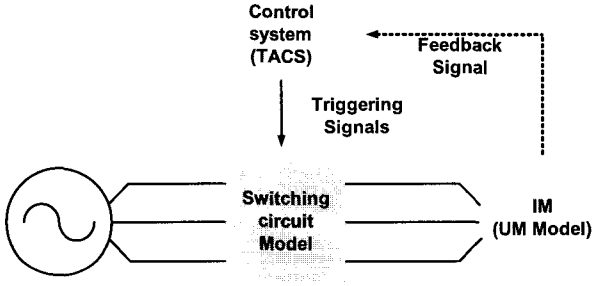

Fig. 3 EMTP structure of ASD system

The switching circuit consists of an uncontrolled diode-bridge rectifier, DC-link, and voltage source inverter. In this paper, the voltage source that is applied to the inverter is assumed as the ideal DC source, which has no ripples. Also, the control system is modeled as the TACS (Transient Analysis of Control System) of EMTP. TACS allows the frequency conversion to be possible as the system generates the trigger signal to control the inverter switch.

The PWM inverter controls the output of the VVVF (Variable Voltage Variable Frequency) and simultaneously maintains constant flux. If the PWM inverter is used in a motor system, speed control is available without any reduction on the efficiency or the power factor of a motor for extensive adjustable speed operation. It is also frequently used in the speed control of an AC motor and maximum torque operation due to the advantages of elimination and reduction of specific harmonics.

The most prevalent advantage of the PWM inverter is that the specific damping filter for reduction of harmonics is not required and is easy to manage as the modified pulse waveform that controls the magnitude of inverter output voltage. However, many harmonics that are generated by the frequent On/Off operation of switching devices can cause power loss, in addition to EMI (electromagnetic interference), noise, and torque ripple [9].

Fig. 4 and Fig. 5 show the phase-to-ground voltage and harmonic spectrum of a PWM 3-level inverter.

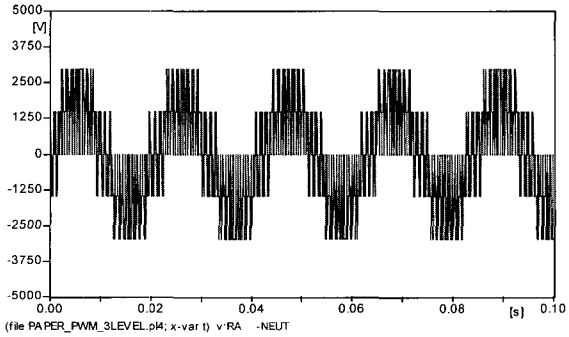

Fig. 4 Phase-to-ground voltage of a PWM 3-level inverter

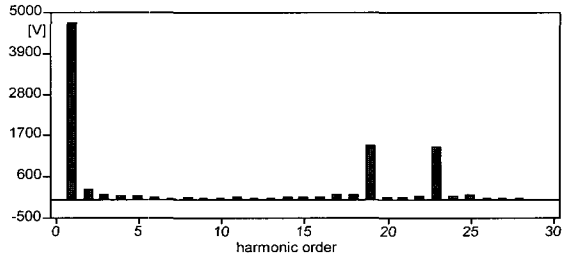

Fig. 5 Harmonic spectrum of a PWM 3-level inverter

The harmonic order h_{PWM} of a PWM 3-level inverter is calculated by Eq. (10)

$$h_{PWM} = n(m_f) \pm k \tag{10}$$

where, h_{PWM}: harmonic order, n: integer, m_f: frequency modulation ratio, and k: side-band.

The harmonics of the PWM inverter appear in the side-band, which centers on a multiple of frequency modulation ratio (m_f). That is, according to the frequency modulation ratio, the odd and even harmonics are combined [9]. When the switching frequency is 1[kHz] and the operation frequency is 47.619[Hz], Fig. 5 indicates the harmonic spectrum of the PWM 3-level inverter. It appears dominantly as the harmonic of the 19th and 23rd order due to m_f=21.

The direct drive method to use a PWM inverter is increasing along with the development of power switching devices and control techniques. As well, the method to apply the multi-level type inverter in the high-voltage induction motor is developing. Representative inverters are the NPC (Neutral-Point-Clamped) inverter, the FC (Flying-

Capacitor) inverter and the H-Bridge cascaded inverter. This paper proposes a systematic approach to reduce the harmonics with a H-Bridge cascaded 7-level inverter among the multi-level inverters. The merits of the H-Bridge cascaded inverter are equal to the power division and the device utilization ratio for driving the high-voltage induction motors [10].

This inverter has the form by which a power cell, consisting of the diode rectifier and 2-level inverter, is connected by series in each phase. DC is the ideal voltage source for the simulation because it sets V_{dc}=900[V]. Fig. 6 and Fig. 7 show the phase-to-ground voltage and the harmonic spectrum of a H-Bridge cascaded 7-level inverter.

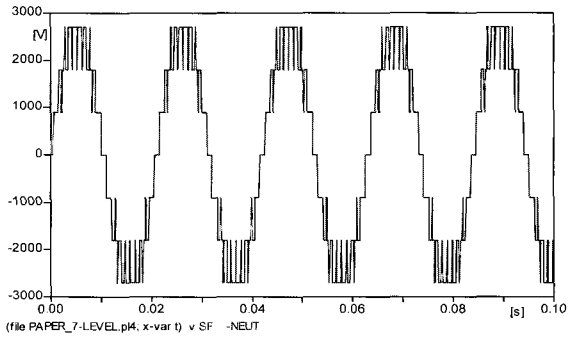

Fig. 6 Phase-to-ground voltage of H-Bridge cascaded 7-level inverter

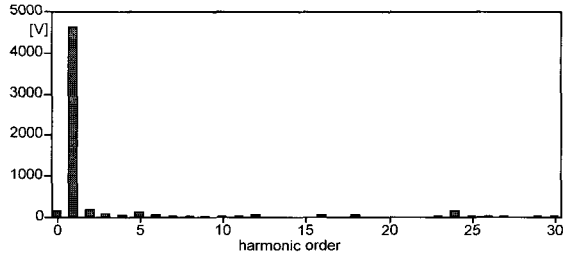

Fig. 7 Harmonic spectrum of H-Bridge cascaded 7-level inverter

When the harmonic spectrum of a H-Bridge cascaded 7-level inverter is compared with Fig. 5, the harmonics of high order are considerably reduced.

4. Comparative Analysis on the Switching Surge Voltage by Drive Form

4.1 Modeling of high-voltage induction motor

This paper uses the U.M (Universal Machine) model of EMTP for modeling the high-voltage induction motor. In this UM model, electrical circuits are represented by d-q axis. Mechanical factors represent factors to be transformed into electrical circuits. Table 1 shows the correlation between the electrical and mechanical fields [8].

The equation of mechanical motion is given by Eq. (11) in the system that combines the electrical field with the mechanical field.

$$T_m = J\frac{d\omega_m}{dt} + D\omega_m + T_e \tag{11}$$

If Eq. (11) transforms into the equation of electrical motion, it becomes Eq. (12).

$$I_m = C\frac{dV_m}{dt} + \frac{V_m}{R} + I_e \tag{12}$$

Therefore, the motor data should be inputted after transforming into the electrical field. If the load toque is transformed into the electrical factor, the motor is negative and the generator is positive [8, 11].

Table 1 Correlation between the electrical and mechanical fields

Mechanical	Electrical
T (Torque on mass)	I (Current into node)
ω_m (Angle Speed)	V (Node voltage)
θ_m (Angle)	Q (Capacitor charge)
J (Moment of inertia)	C (Capacitance to ground)
K (Spring constant)	Y_L (Reciprocal of Inductance)
D (Viscous Damping)	Y_R (Conductance)

Table 2 is the parameter of a high-voltage induction motor for modeling.

Table 2 Parameter of 3 phase squirrel induction motor

rating	1.5[MW], 3.3[kV], 6P, 60[Hz], Y-connected	
parameter	stator resistance	0.341368[Ω]
	rotor resistance	0.112588[Ω]
	stator leakage inductance	0.001543[H]
	rotor leakage inductance	0.001543[H]
	mutual inductance	0.02987[H]
moment of inertia	78.5[kg·m^2]	

4.2 Comparative analysis for switching surge voltage by drive form

Fig. 8 and Fig. 9 present the results that compare the voltage measured at the output terminal of the inverter and the input terminal of the induction motor.

Fig. 8 illustrates the output voltage of the inverter and the input voltage of the induction motor driven by the PWM 3-level inverter. If the output voltage of the inverter is 1[P.U.] the voltage that is applied to the induction motor

results in an overvoltage of nearly 2[P.U.]. Such overvoltage puts excessive strain on the stator winding and becomes the major cause of insulation failure. In particular, the input voltage, which is the overvoltage of 2[P.U.] has a severe effect on the insulation of the induction motor because it takes place on a periodic basis.

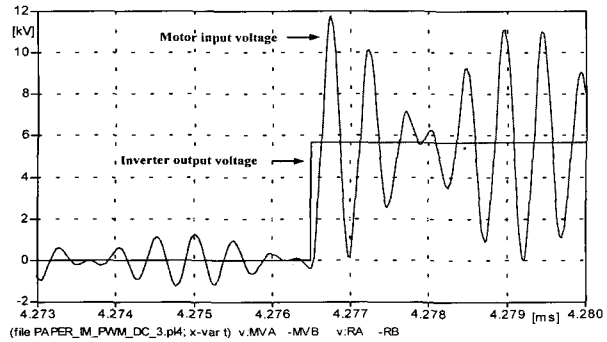

Fig. 8 Output voltage of inverter and input voltage of induction motor using PWM 3-level inverter

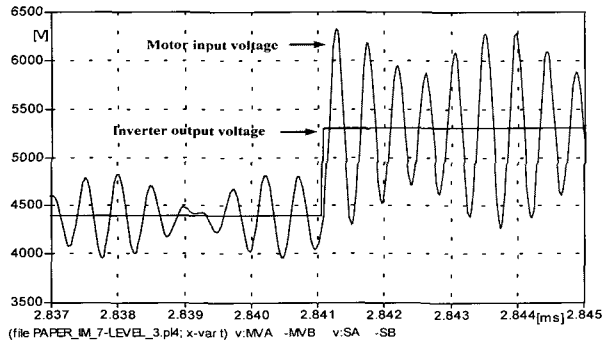

Fig. 9 Output voltage of inverter and input voltage of induction motor using a H-Bridge cascaded 7-level inverter

Fig. 9 shows the output voltage of the inverter and the input voltage of the induction motor using the H-Bridge cascaded 7-level inverter. The input voltage of the motor is an overvoltage of 1.2[P.U.] in comparison with the output voltage of the inverter. When a H-Bridge cascaded 7-level inverter is used, the switching surge voltage is considerably reduced because the rate of voltage rise (*dv/dt*) is lowered by the voltage.

5. Analysis on the Switching Surge Characteristics of High-voltage Induction Motor Fed by Inverter

This paper presents the system equivalent model so that the characteristics of switching surge can be analyzed.

Fig. 10 shows the system equivalent model. The presented model of the inverter-cable-motor consists of a steep pulse source, distributed circuit and surge impedance of the motor.

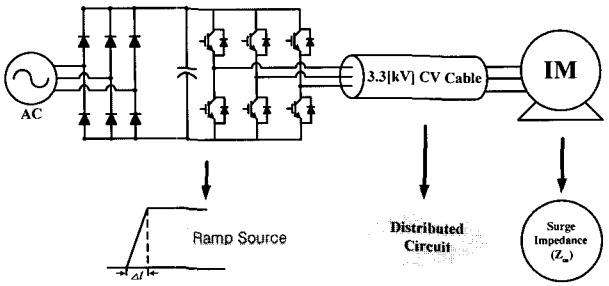

Fig. 10 System equivalent model

5.1 Modeling of steep pulse source

The output waveform of the PWM inverter occurs as a train of wavefronts with sharp rise-time. Hence, the steep pulse source can be simply modeled as one wavefront. This paper uses EMTP Type 12 ramp source for modeling the typical wavefront of the PWM inverter. Generally, the switching frequency of the IGBT switching device is 2~20[kHz] and the rise-time is 50~400[ns] [7]. Fig. 11 indicates the voltage waveform in the event of rise-time t_r=0.2[μs].

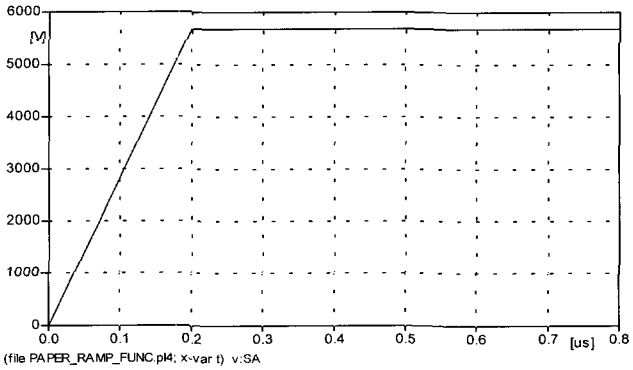

Fig. 11 Voltage waveform in the case of rise-time t_r=0.2[μs]

5.2 Calculation of cable constant

For the transient analysis of switching surge voltage, a cable is modeled as a distributed circuit and a cable constant must be calculated as MHz range frequencies that correspond to rise-time of μs. For example, if the rise-time of the wavefront is 0.1[μs], the cable constant must be calculated as 1[MHz] frequency [1].

The LCC (Line/Cable Constants) program of ATPDraw, which is a graphical user interface for EMTP, can calculate the cable parameters for assigned frequency on the basis of the geometrical structure and physical data of the cable. Then, the cable distributed parameter is calculated by high-frequency corresponding to the rise-time of the PWM pulse. The geometrical structure and physical data of the cable use the standard of KS C 3131, 3.3[kV] CV cable (CV

cable: Cross linked polyethylene insulated cable). Fig. 12 and Fig. 13 show the structures of 3.3[kV] SC CV cable (100 mm^2) and 3.3[kV] 3C CV cable (100 mm^2).

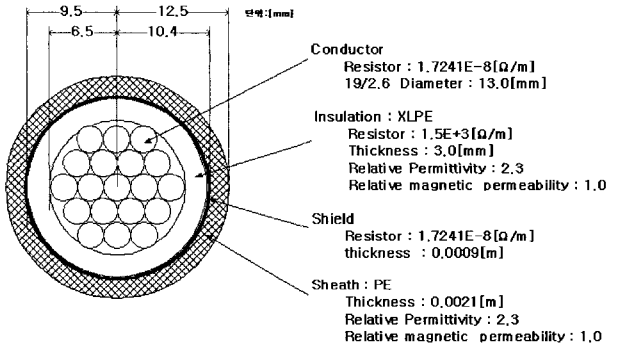

Fig. 12 3.3[kV] SC CV cable (100 mm^2)

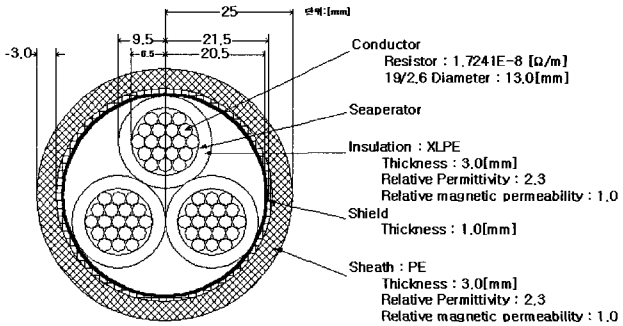

Fig. 13 3.3[kV] 3C CV cable (100 mm^2)

5.2 Surge impedance of motor

Usually, the capacitance of the stator winding increases and the inductance of the motor decreases while the machine rating becomes higher [3]. Therefore, if a motor is large, the surge voltage is small because the surge impedance of the motor is small. The surge impedance of the motor is calculated by Eq. (3).

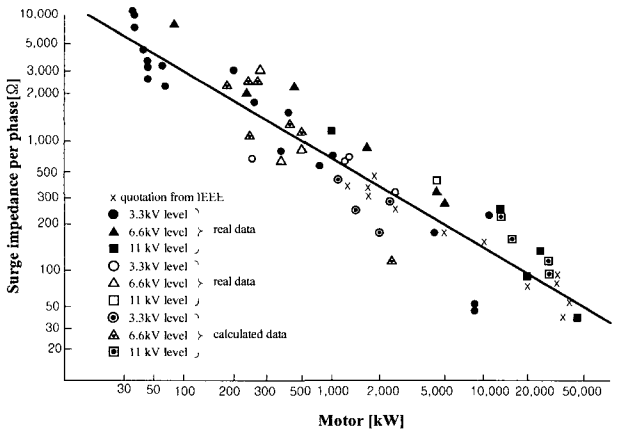

Fig. 14 Surge impedance vs. motor size

This paper quotes the surge impedance from a report by KEPRI, "A study on the reduction method and the analysis of VCB switching surge for the high voltage induction motor"[12]. Therefore, we determine that the surge impedance is 500[Ω] at each phase of the induction motor.

6. Case study

Based on the proposed equivalent model and parameter estimation technique, EMTP analysis is performed in order to investigate the characteristics of switching surge voltage. Cable structures and cable burial depths are applied to study an external influence in the motor system. As such, cable structures of single core and triple core, and cable burial depths of 0.6[m] and 1.2[m] are applied. Moreover, various rise-times and cable lengths are applied to analyze the correlation of PWM inverter rising time and the length of feeder cable between PWM inverter output and induction motor input. Rise-times of 20[ns], 50[ns], 100[ns], 200[ns], and 400[ns], and cable lengths of 5[m], 10[m], 50[m], 100[m], 200[m], 300[m], and 500[m] are applied. EMTP analysis doesn't perform in the case of a motor system without feeder cables because the high-voltage inverter cannot directly connect to the induction motor and a variation of surge doesn't occur at the input terminal of the induction motor.

6.1 3.3[kV] SC CV Cable

As a case study, the rise-time of steep pulse and cable length were set at 0.2[ns] and 100[m] respectively, with a horizontal cable arrangement as shown in Fig. 15. Fig. 16 indicates the output waveform example of a system equivalent model.

When $V_{dc} = 5672.5[V]$ is set to be 1[P.U.], Fig. 17 shows the distribution of switching surge voltage depending on the rise-times of steep pulse and cable lengths.

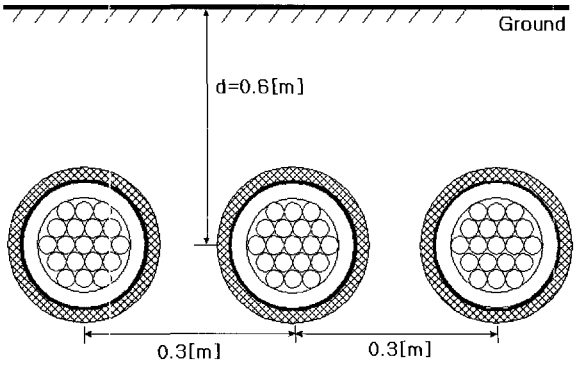

Fig. 15 Horizontal arrangement of 3.3[kV] SC CV cable

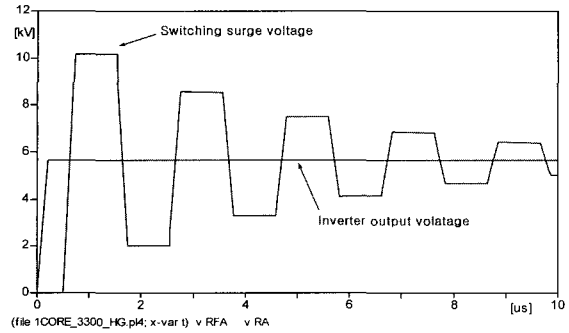

Fig. 16 Example of output waveform

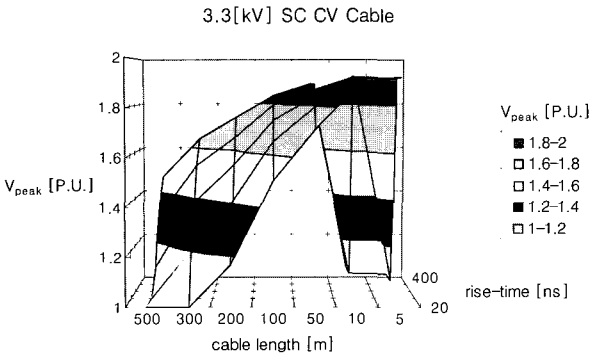

(a)

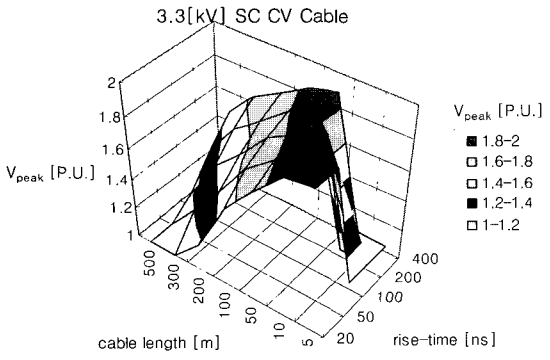

(b)

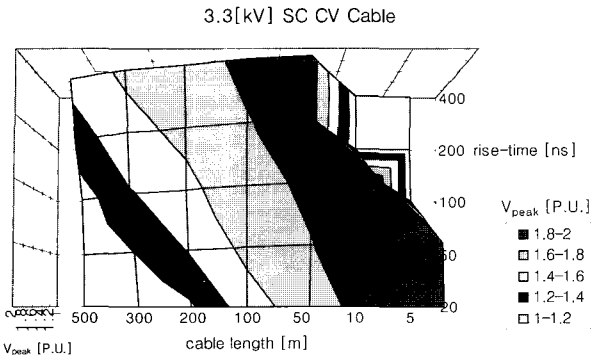

(c)

Fig. 17 Distribution of switching surge voltage using 3.3[kV] SC CV cable

The results that are simulated by the following cases are depicted in Fig. 17. Cable burial depths of 0.6[m] and 1.2[m], and the cable arrangement of vertical, triangular (symmetry, asymmetry) and pipe-type are applied. We arranged the cable on the ground as well. This result came about because the switching surge voltage is influenced on the propagation velocity, which is calculated by the relative permittivity of XLPE.

6.2 3.3[kV] 3C CV cable

Fig. 18 indicates the arrangement of 3.3[kV] 3C CV cable.

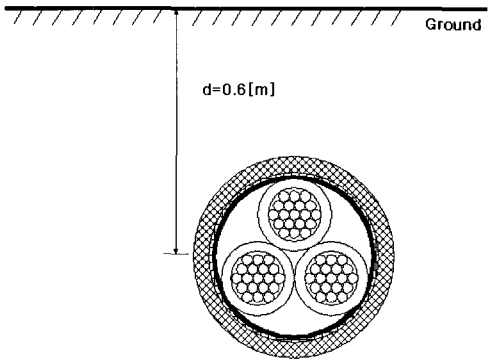

Fig. 18 3.3[kV] 3C CV cable arrangement

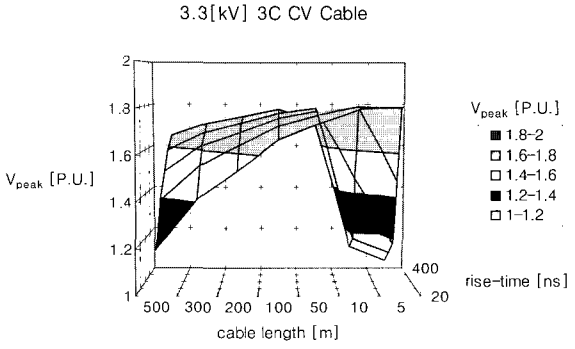

(a)

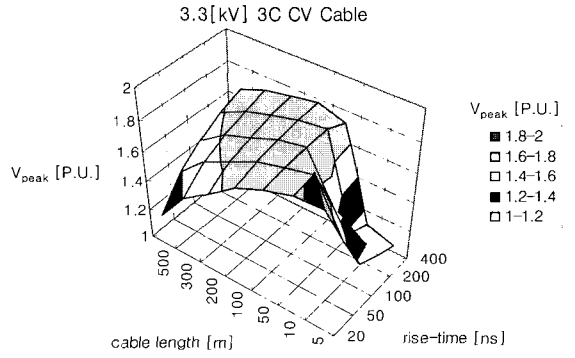

(b)

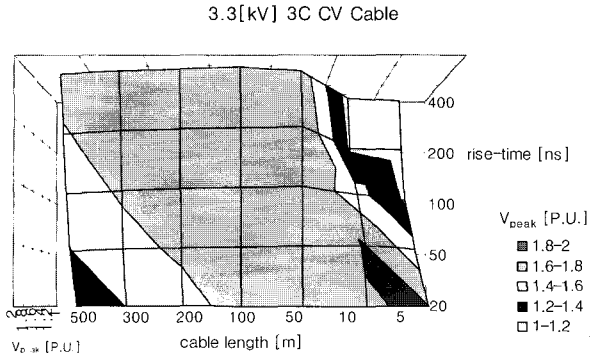

(c)

Fig. 19 Distribution of switching surge voltage using 3.3[kV] 3C CV cable

Fig. 19 displays the distribution of switching surge voltage depending on the rise-times of steep pulse and cable lengths. When compared with 3.3[kV] SC cable, the switching surge voltage is low on the average due to the cable structure.

The results simulated by the following cases are illustrated in Fig. 19. Cable burial depths of 0.6[m] and 1.2[m], and the cable arrangements of vertical, triangular (symmetry, asymmetry) and pipe-type are applied. We arranged the cable on the ground as well.

7. Conclusion

In this paper, the characteristics of switching surge of a high-voltage induction motor fed by a PWM inverter are analyzed. In order to examine the characteristics of switching surge, the system equivalent model is proposed and EMTP analysis is performed

The results are presented as follows:

1. If the surge impedance of the motor is high, the input voltage of the motor is nearly double because the reflection coefficient is high.
2. The faster the rise-time of the inverter is, the higher the magnitude of switching surge voltage is.
3. The switching surge voltage has the critical length, which generates an overvoltage.
4. The switching surge voltage is influenced by the geometrical structure of the cable and the relative permittivity of the cable insulator, but it isn't influenced by a cable burial depth and a cable arrangement.

When a manufacturer designs a high-voltage induction motor fed by an inverter, the manufacturer must carefully consider the switching surge voltage because it has such great effect on the stator winding of the motor. Taking this consideration into account, the rise-time of the inverter and the length and structure of the cable were chosen because the insulation design of the motor is the significant factor related to the life span of the motor. Consequently, it is necessary to improve the insulation capability of the high-voltage induction motor fed by a high speed switching inverter to be able to endure the switching surge voltage.

Acknowledgements

This work was supported by the Korea Energy Management Corporation (KEMCO).

References

[1] H.A. Toliyat, G. Suresh, A. Abur, "Simulation of Voltage Stress on the Inverter Fed Induction Motor Winding Supplied Through Feeder Cable", Industry Application Conference, Thirty-Second IAS Annual Meeting, IAS '97, Vol. 1, pp.143-150, 1997.

[2] L. Gubbala, A. Von Jouanne, P.N Enjeti, C. Singh, H.A Toliyat, "Voltage Distribution in the Windings of an AC Motor Subjected to High dv/dt PWM Voltages", Power Electronics Specialists Conference, 1995. PESC '95, 26th Annual IEEE, Vol. 1, pp.579-585, 1995.

[3] Christopher J. Melhorn, Le Tang, "Transients Effects of PWM Drives on Induction Motors", IEEE Transactions on Industry Applications, Vol. 33, No. 4, pp.1065-1072, July/August 1997.

[4] Seung-Yeop Song, Jae-Chul Kim, Do-Hoon Lee, Jung-Eun Shin, Tae-Hoon Im, "The Analysis for the Characteristics of Switching Surge of Adjustable Speed Drive by Inverter", KIEE Summer Conf., pp. 241-243, 2003.7.

[5] Erik Persson, "Transient Effect in Application of PWM Inverters to Induction Motor", IEEE Transaction on Industry Application, Vol. 28, No. 5, pp.1095-1101, September/ October 1992.

[6] J.C. Das, "Power System Analysis", Marcel Dekker INC, 2002.

[7] Annette von Jouanne, Dudi A. Rendusara, Prasad N. Enjeti, James Will Gray, "Filtering Techniques to Minimize the Effect of Long Motor Leads on PWM Inverter-Fed AC Motor Drive Systems", IEEE Transactions on Industrial Application, Vol. 32, No. 4, pp.919-926, July/August 1996.

[8] ATP Rule Book, ATP solford Version of EMTP, Vols. 1, 2, Leuven EMTP Center, 1987.

[9] Jong-Gyeom Kim, Eun-Woong Lee, "The Effect and Harmonics Generating by Inverter Types of

Adjustable Speed Drives of Induction Motor", KIEE Trans., Vol. 47, No. 7, pp.906-913, 1998. 7.

[10] Muhammad H. Rashid, "Power Electronics Handbook", Academic Press, 2001.

[11] Seung-Yeop Song, Jae-Chul Kim, Do-Hoon Lee, Jung-Eun Shin, Kwang-Hyun Noh, "The Analysis for the Effect of Switching Surge of Induction Motor using EMTP", KIEE Autumn Conf., pp.278-280, 2003.11.

[12] Eun-Woong Lee, Jong-Gyeom Kim, Taek-Soo Kim, Wook-Dong Kim, Kwang-Hoon Kim, "A Study on the Reduction Method and the Analysis of VCB Switching Surge for High Voltage Induction Motors", KEPRI, DEC. 1993.

Jae-Chul Kim

He received his B.S. degree in Electrical Engineering from Soongsil University, Korea, in 1979. He received his M.S. and Ph.D. degrees in Electrical Engineering from Seoul National University, Korea, in 1983 and 1987. He has served as a Professor of Electrical Engineering at Soongsil University since 1988. His research interests are in the areas of power systems, power quality and reliability, distribution system operations and power facilities diagnosis.

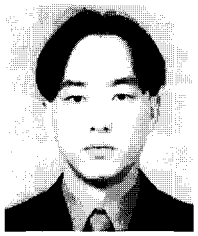

Seung-Yeop Song

He received his B.S. and M.S. degrees in Electrical Engineering from Soongsil University, Korea, in 2002 and 2004. His research interests are in the areas of power systems and power facilities diagnosis.

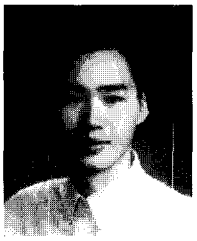

Do-Hoon Lee

He received his B.S. and M.S. degrees in Electrical Engineering from Soongsil University, Korea, in 2002 and 2004. He is currently working at the Electro-technology R&D Center of LG Industrial Systems. His research interests are in the areas of power systems, power facilities diagnosis and system reliability.